Greenhouse Gases: Science and Technology, Volume 8, Issue 6, December 2018, pp. 1124-1133
DOI:10.1002/ghg.1825

CO_2 capture and attrition performance of competitive eco-friendly calcium-based pellets in fluidized bed

Chenglin Su [a], Lunbo Duan *[a], Edward John Anthony [b]

[a] Key Laboratory of Energy Thermal Conversion and Control, Ministry of Education, School of Energy and Environment, Southeast University, Nanjing 210096, China

[b] Centre for Combustion and CCS, School of Energy, Environment and Agrifood, Cranfield University, Cranfield, Bedfordshire MK43 0AL, UK

Abstract

The incorporation of spent bleaching clay (SBC) into the CaL process has been proposed to reduce the system cost, whereby fuels and/or heat from different SBC regeneration could be used as a partial energy source for the calciner; the regenerated SBC residues are used with lime powders to synthesize pellets. In this paper, the prepared sorbents doped with regenerated SBC and cement were tested in a bubbling fluidized bed (BFB) to further examine the cyclic CO_2 capture capacity and attrition properties. The results revealed that the cyclic CO_2 capture capacity of pellets modified by pyrolyzed SBC and/or cement displayed significantly better performance than limestone, consistent with the thermogravimetric analyzer (TGA) results. This is due to the improvement of pore structure and better sintering resistance produced by adding inert phases to the sorbent. The elutriation rates of the composites prepared with pyrolyzed SBC and/or cement were consistently lower than for crushed limestone. Scanning electron microscopy (SEM) images indicated that the pellets possessed higher sphericity than limestone particles, reducing surface abrasion. Limestone exhibited a high attrition rate (diameter reduction rate) of 10.7 μm/cycle, which could be effectively eliminated by adding regenerated SBC and/or cement. "L-5PC-10CA" (85% lime/5% pyrolyzed SBC/10% cement) showed a higher attrition resistance, exhibiting the lowest attrition rate of 7.9 μm/cycle. Based on the analysis

of breakage and probability density function (PDF) for particle size distribution, it appeared that pellets without cement experienced breakage (mostly chipping and disintegration) and surface abrasion, while "L-10CA" (90% lime/10% cement) and "L-5PC-10CA" mainly suffered only surface abrasion, combined with some chipping.

Keywords: CO_2 capture; calcium looping; CaO-based sorbent; spent bleaching clay regeneration; attrition

***Corresponding Author at:** 2 Sipailou, School of Energy and Environment, Southeast University, Nanjing 210096, China. Tel: +86 25 83790147.

E-mail: duanlunbo@seu.edu.cn

1. Introduction

Calcium looping (CaL), one of the promising post-combustion CO_2 capture technologies, can be easily integrated with existing energy-intensive plants. CaL removal of CO_2 from coal-fired power plant flue gas has already been demonstrated at pilot scale (0.1-2 MW)[1–4]. Furthermore, CaL-steel plant[5] and CaL-cement plant[6–9] have been proposed to reduce CO_2 emissions in steel and cement production and reduce overall costs for both processes. In addition, the CaL process is likely to play a role in energy storage[10]. Due to the advantages of high energy density and long storage duration, chemical heat storage has attracted considerably more interest than thermal energy storage methods, i.e., sensible and latent heat storage. The reverse reaction of CaO + CO_2 appears to be one of the best candidates for storing high-temperature energy[11]. The CaL process, acting as energy storage for power plants, would also increase power generation flexibility[10]. Recently, the integration of CaL and a concentrating solar power plant, i.e., CaL-CSP plant, has generated much interest[12,13], as the CaO/CO_2 system has a higher energy density of around 3.2 GW/m^2 compared to that of molten salts (about 0.8 GW/m^2) used in the existing plants.

Natural CaO-based inorganic materials, like limestone and dolomite, are inexpensive, non-toxic and abundantly available, which lead to reduced costs for the CaL process. However, although CaL has a lower efficiency penalty of 6-8% points, compared to those of amine scrubbing and oxy-combustion technologies, the high energy penalty of conventional CO_2 capture systems still results in higher fuel consumption and costs. Based on previous modelling results, the CO_2 capture cost is estimated to be \$29-50/t CO_2, which is less than half that for amine scrubbing[14,15]. More importantly, to further reduce the cost of sorbents, several types of

waste-derived CaO-based materials have been tested in CaL cycles. Calcium-containing solid wastes such as carbide slag[16–18], lime mud[19], iron and steel slag[20,21], have been examined as potential CaO sorbents. Moreover, alkali silicate-based materials including fly ash (FA) from fossil fuel combustion[22,23], rice husk ash[24,25], etc., were used to modify natural limestone to enhance the cyclic performance.

Spent bleaching clays (SBC) containing oil and inorganic components (mainly SiO_2 and Al_2O_3) are produced from the oil refining process. In the work of Su et al.[26], a novel system integrating CaL with SBC was proposed for the first time. In this system, the energy recovered from SBC could supply the needs of the calciner; and the pyrolyzed and/or organic solvent extracted SBC containing combustible content and inert phase could be used to synthesize limestone-based sorbent. Pelletization methods were used to prepare the composite. Doping the limestone powder with support and pore-forming materials can also be done in the pelletization process. Cement as support was determined to be competitively favorable[27–29]. Another advantage of the method is that pellets with desirable particle size and shape can be formed for use in real fluidized bed systems. Cyclic performance tests of synthesized pellets doped with regenerated SBC and cement have been performed in a thermogravimetric analyzer (TGA) apparatus, the results of which revealed that these lime-based pellets possessed higher specific surface area and pore volume due to the oxidation of combustible content inside, which contributed to better CO_2 capture performance.

Apart from the carbonation activity, the attrition issue is another major challenge for the application of sorbents in the CaL process. The particles will experience breakage and abrasion in the fluidized bed, which causes the loss of sorbent and increases the relative cost. In this paper, the cyclic carbonation performance and attrition properties of the prepared pellets doped with regenerated SBC and cement were assessed in detail using a bubbling fluidized bed.

2. Experimental section

2.1 Materials and sorbent preparation

The spent bleaching clays from the lubricating oil refining process were supplied by Sinopec Corp., China. The average oil content left in the SBC was determined to

be 26.3% from the calcination process. X-ray fluorescence (XRF) measurements showed that SiO_2 and Al_2O_3 were the main inorganic components in calcined SBC. The relevant methods used and the results of these tests are discussed in detail elsewhere[26].

In view of the simplicity of the pyrolysis regeneration process and the improvements in CO_2 adsorption performance of sorbents modified by pyrolyzed SBC, this material was used to prepare lime-based pellets in this paper. The pelletization was performed in a laboratory mechanical granulator (Xiyite G6, China). Mixing powders consisting of calcined limestone, regenerated SBC and/or cement were agitated by a high-speed agitator and chopper, and deionized water was sprayed on the mixture to initiate bonding and pelletization. The detailed pelletization process is described elsewhere[30].

A range of sorbent pellets was synthesized using various materials, the compositions of which are summarized in Table 1. The prepared sorbents are denoted as L-αPC-βCA, where L, PC and CA refer to calcined limestone, pyrolyzed SBC and cement, respectively; α and β refer to the doping ratios (0, 5 or 10 wt.%). For comparison, raw limestone particles and pure calcined limestone pellets were also examined to determine the effect of pelletization on sorbent performance. These pelletized materials are designated as "L" and "LP", respectively.

Table 1: Compositions of materials used in preparation of different samples.

Sample	Lime (wt.%)	Pyrolyzed SBC (wt.%)	Cement (wt.%)
L	100	0	0
LP	100	0	0
L-10PC	90	10	0
L-10CA	90	0	10
L-5PC-10CA	85	5	10

2.2 Bubbling fluidized bed test

Multiple calcination/carbonation reaction cycles were performed in a laboratory bubbling fluidized bed (BFB) unit, shown in Figure 1. A quartz tube (25 mm i.d., 1100 mm height) was used as the reactor, consisting of a preheating section (600 mm in height) and a reaction section (500 mm in height). The gas distributor is a sintered

glass disk plate. The fluidized gases, metered by mass flow controllers, were mixed in a gas mixer before being introduced from the bottom of the tube. A nondispersive infrared gas analyzer (ThermoFisher, Antaris IGS) was used to measure the CO_2 concentration in the outlet gas after filtering in real time.

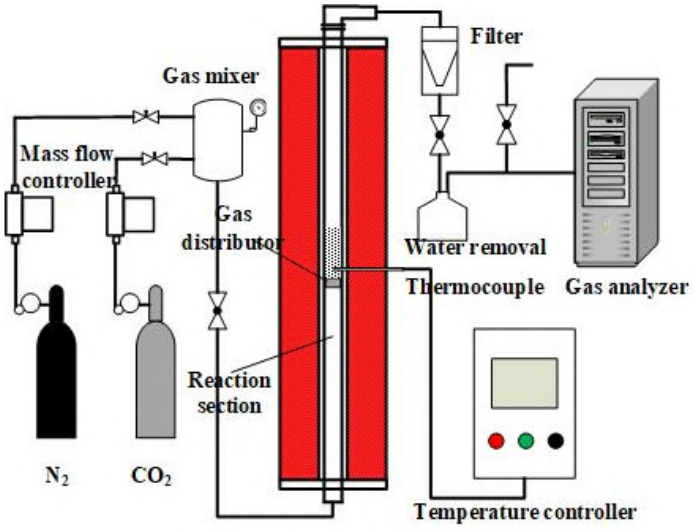

Figure 1. Schematic of the bubbling fluidized bed.

Carbonation performance

The sorbent pellets were pretreated as follows: a batch of pellets in the size range of 0.25-0.6 mm was loaded into the reactor and subjected to complete carbonation in 20% CO_2/80% N_2 at 650 □ for 1 h, at a gas velocity of 0.05 m/s. After discharge from the bubbling fluidized bed, the pellets in the size range of 0.3-0.5 mm were sieved and used in the tests. 15 g pellets without inert bed material were employed for each test. Experiments were typically carried out at atmospheric pressure. The calcination stage was in 80% CO_2/20% N_2 at 920 □ for 15 min, and carbonation conditions were 15% CO_2/85% N_2 at 650 □ for 25 min. In the first cycle, all sorbents were heated in air from ambient temperature to 920 □ for oxidation of combustible components. After calcination, the temperature was lowered to 650 □, switching to pure N_2 atmosphere simultaneously to avoid premature carbonation. All sorbents were subjected to 20 reaction cycles in each trial.

The sorbent reactivity was assessed by the cyclic CO_2 uptake, calculated by Eqn. (1) as follows:

$$X_N = \frac{\int_0^t Q[\varphi_{CO_{2,0}}(t) - \varphi_{CO_2}(N,t)]dt}{22.4 m_{cal} / M_{CO_2}} \quad (1)$$

where X_N represents the cyclic CO_2 uptake of samples after N cycles, g(CO_2) g(calcined sorbent)$^{-1}$; t is carbonation time, min; N represents number of reaction

cycles; Q is volume flow rate, L·min^{-1}; $\varphi_{CO_2,0}$ (t) denotes CO_2 concentration at the outlet in the absence of sorbent at t min, vol.%; φ_{CO_2} (N, t) represents CO_2 concentration in the presence of sorbent at t min, vol.%; m_{cal} is the mass of calcined sorbent, g; and M_{CO_2} is the molecular weight of CO_2, g·mol^{-1}.

Attrition performance

The attrition properties of prepared pellets and limestone particles were examined in the BFB tests. During the multiple cycles, the fines escaping from the reactor were captured by a fiber filter located at the reactor outlet, as shown in Figure 1. In order to prevent hydration and recarbonation of the collected fines, the filter was put in a drier as soon as possible after the completion of a test. Then the mass of particles elutriated was determined by the difference in fiber filter weights before and after each test, and the elutriation rate at a given velocity was calculated by Eqn. (2). Each trial was duplicated under the same experimental conditions.

$$E = (m_t - m_f) / m_0 \tag{2}$$

Here m_t is the total mass of used filter after cycles; m_f is the mass of fresh filter; m_0 is the total mass of given sorbents at the start of the test.

After each long-cycle test, the particles in the bed were discharged and sieved using a sieve shaker with 8 sieves plus the bottom tray to determine the particle size distribution (PSD). The PSD of the entire sample (elutriated + remaining in bed) after the experiment was used to identify the attrition mechanisms. The probability of pellet breakage was measured by "fragments", meaning the particles whose size falls below the lower limit of the feed size interval (i.e., 0.3 mm in this study). The definition of breakage probability (f) is as shown in Eqn. (3):

$$f = \frac{m_{Fragments<0.3mm}}{m_{total\ mass\ in\ the\ beginning}} \tag{3}$$

Here, the Sauter average particle diameter (d_{sv}) was used to determine the particle size of sorbent before and after reaction, which is calculated by Eqn. (4). The attrition rate (R_N) reflects the attrition performance of sorbent, as defined by Eqn. (5):

$$d_{sv} = \frac{1}{\sum_i x_i / d_{pi}} \tag{4}$$

$$R_N = \frac{d(d_{sv,N})}{dN} \bullet 1000 \tag{5}$$

where x_i is the mass fraction of particles in size interval i; d_{pi} is the length of size interval i; and $d_{sv,N}$ is Sauter mean diameter of sorbent after N cycles, mm.

The particle size distribution of the elutriated fines for different sorbent pellets was measured using a Malvern Mastersizer 2000 instrument by laser diffractometry of the samples dispersed in absolute ethyl alcohol. The surface morphology of the pellets before and/or after cyclic reactions was investigated by a scanning electron microscope (SEM, Hitachi S-4800, Tokyo, Japan).

3. Results and discussion

3.1 Effect on CO_2 capture performance of sorbents

To demonstrate the experimental reproducibility, each single carrying capacity test in this paper was carried out in duplicate, and the averaged results are presented. Based on TGA test results[26], regenerated SBC and cement were chosen as dopants. Figure 3 illustrates the CO_2 concentration curves during the 1st and 20th carbonation stage for different doped sorbents in the BFB tests. Clearly, there is a fast reaction stage and a slow one for each sample in the initial reaction cycle. A minor difference in the duration of the fast stage was observed, referring to the initial 700 seconds in Figure 3. However, the total duration of carbonation reaction for "L-10PC" and "L-5PC-10CA" was around 1400 sections, longer than 1200 seconds of "L". It appears that the wider pore area and volume distribution in pore size range of 10-100 nm (seen in Fig. 5 in ref.[26]) contributed to the prolonged slow reaction stages for both "L-10PC" and "L-5PC-10CA".

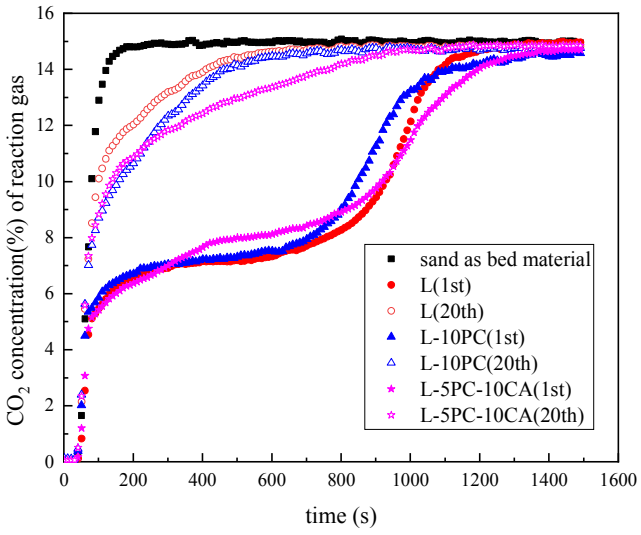

Figure 3. CO_2 concentration curves during the 1st and 20th cycles for several sorbents.

The cyclic CO_2 uptake for the synthesized pellets compared to natural limestone

particles in the BFB tests is illustrated in Figure 4. It can be seen that all pellets performed better than the original limestone after the 1st cycle. After 20 cycles, the CO_2 uptake of four samples increased from 0.095 to 0.206 g(CO_2) g(calcined sorbent)$^{-1}$ for the initial limestone and "L-5PC-10CA", respectively. Here, the data have not been corrected for mass loss owing to the elutriation of fines. As presented in Figure 4a, "L-10PC" showed an improvement of 36.8% over that of "L" for the capture capacity after 20 cycles. "L-10CA" exhibited double the carrying capacity in the 20th cycle. It can be recognized that doping pyrolyzed SBC or cement to lime-based sorbents produces a significant effect on enhancing the CO_2 capture performance of CaO sorbents. The BET surface area and BJH pore volume of all sorbents were measured by N_2 physisorption analysis, and are given in Table 2. The specific surface areas were 12.47 and 17.62 m^2 g^{-1} for "L-10PC" and "L-10CA", respectively, which for "L" was just 9.13 m^2 g^{-1}. A similar tendency for the specific pore volume was observed. "L-5PC-10CA" showed the largest pore characteristic values. In addition, it has been confirmed that the thermally stable larnite (Ca_2SiO_4) and mayenite ($Ca_{12}Al_{14}O_{33}$) formed inside improved the sintering resistance of sorbents in our previous paper[26].

Table 2: Porosity characterization of five pellet types

Sample	BET Surface Area (m^2/g)	BJH Pore Volume （cm^3/g）
L	9.13	0.055
LP	11.02	0.076
L-10PC	12.47	0.103
L-10CA	12.62	0.092
L-5PC-10CA	13.74	0.110

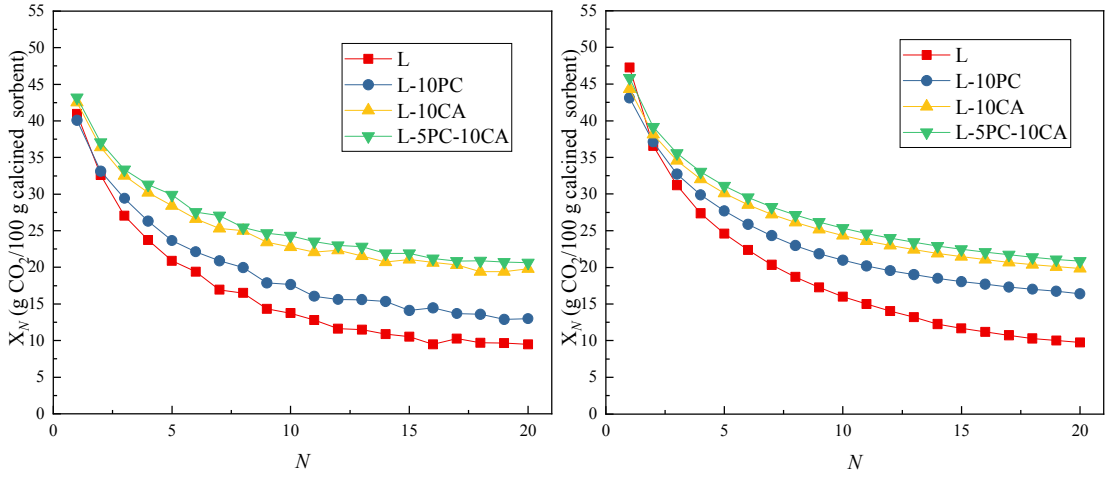

(a) in BFB (b) in TGA

Figure 4. Cyclic CO_2 uptake of doped sorbents through 20 cycles.

The relevant TGA experimental results are given for comparison, in Figure 4b. It should be pointed out that the average CO_2 uptake along 20 cycles in the BFB tests were lower than those observed in the TGA experiments. Figure 5 displays the difference in average CO_2 uptake from the two types of experiments. It is revealed that the average CO_2 uptake in the initial 5 cycles (BFB) was lower by 2.9% and 13.1% for "L-5PC-10CA" and "L", respectively, compared to the TGA test results. This appears to be due to the sorbent losses caused by elutriation and greater diffusion resistance by larger particle size. By contrast, the drop in the degree of average CO_2 capture capacity in the last 5 cycles was reduced by a significant extent. It should be noted that new reaction surface must be produced by attrition, which contributes to improving carbonation. Especially, "L-5PC-10CA" exhibited the lowest drop on average CO_2 uptake.

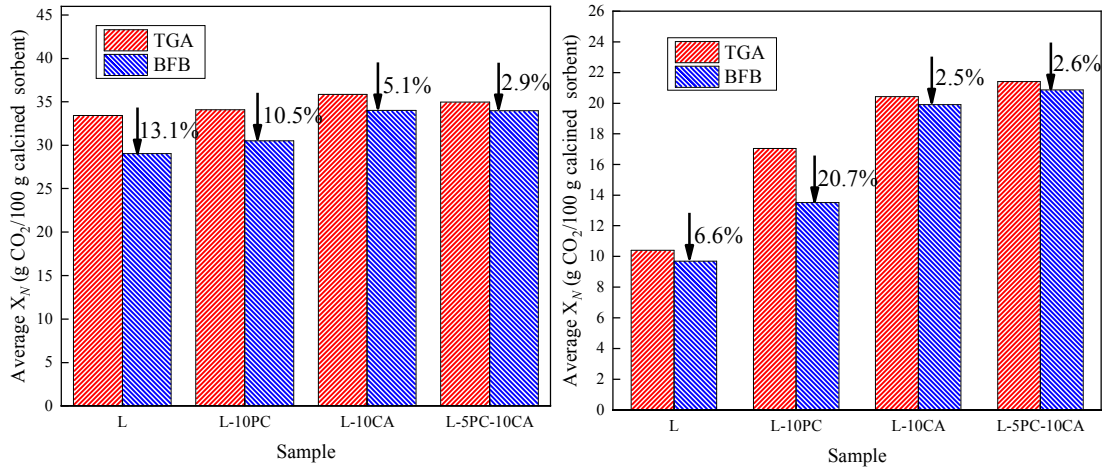

(a) initial 5 cycles (b) last 5 cycles

Figure 5. Comparison of average CO_2 uptake from different experimental methods.

3.2 Effect on attrition of sorbents

Elutriation rate

The fines produced by abrasion are elutriated when the superficial gas velocity exceeds their terminal velocity. The elutriation rate (*f*) for each trial is reported in Figure 6. The losses for all samples were: 4.54 ± 0.76%(L), 3.86 ± 0.63%(LP), 3.45 ± 0.8%(L-10PC), 2.05 ± 0.54%(L-10CA), 2.29 ± 0.58%(L-5PC-10CA). It is clear that the elutriation losses of all modified pellets were lower than for crushed limestone. Attrition by abrasion depends on the resistance of the sorbents to surface wear. Manovic and Anthony[31] reported that cement doping of lime-based sorbent could form a stable $CaO\text{-}Al_2O_3$ framework to strengthen the particle structure. This is consistent with the fact that Ca_2SiO_4 was generated in "L-10PC", in our previous work[26], and must have played a role in causing higher attrition resistance for this pellet. It is generally reported that the attrition rate of fresh $CaCO_3$-based particle is greatest in the initial stage[32]. This is because irregular particles with rough and jagged edges suffer abrasion before being rounded off. The SEM images presented in Figure 7 show that most of the tested natural limestone particle exhibited rather irregular shape, while masses of the manufactured pellets like "L-10CA" and "L-10PC" have better sphericity, which reduced the possibility of surface wear.

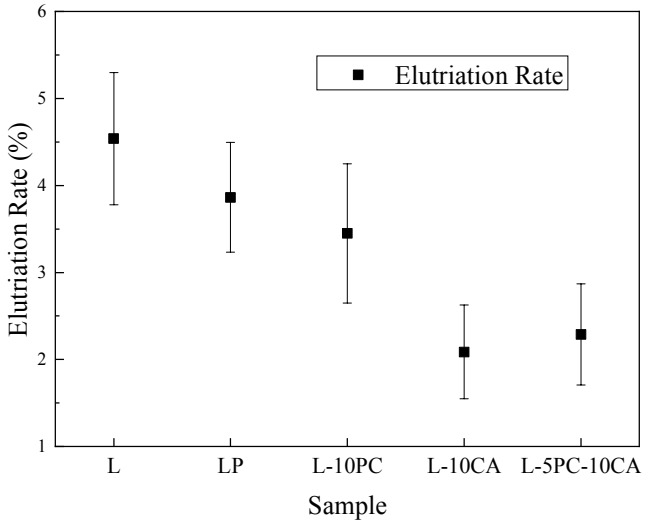

Figure 6. Elutriation rate of five sorbents after 20 cycles.

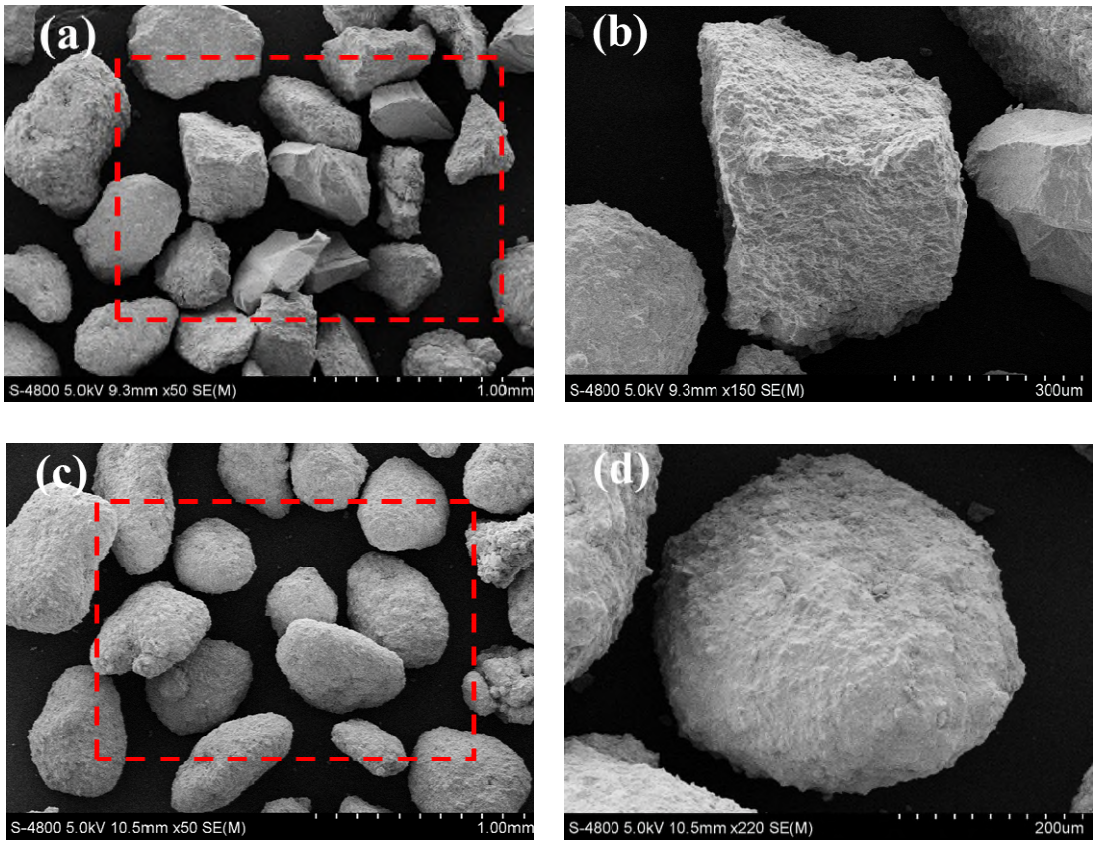

Figure 7. SEM images of "L" and "L-10CA" after 20 cycles: (a), (b) "L"; (c), (d) "L-10CA".

Particle size distribution (PSD)

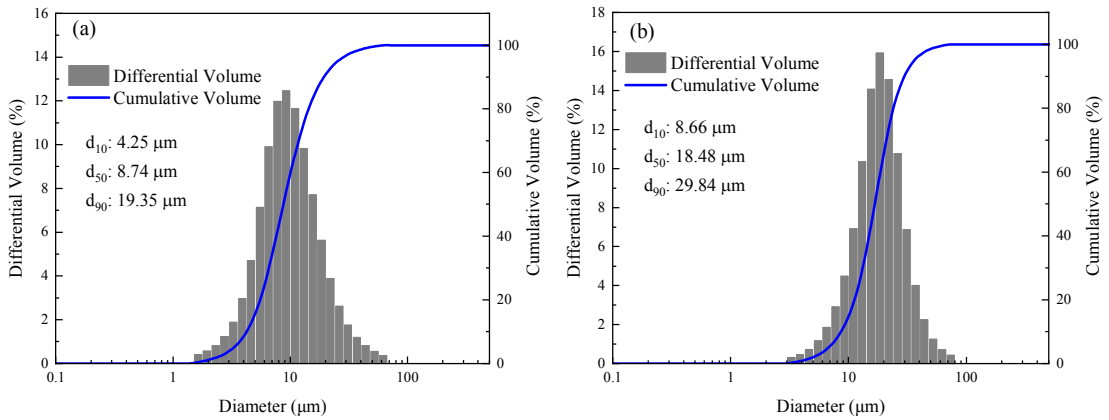

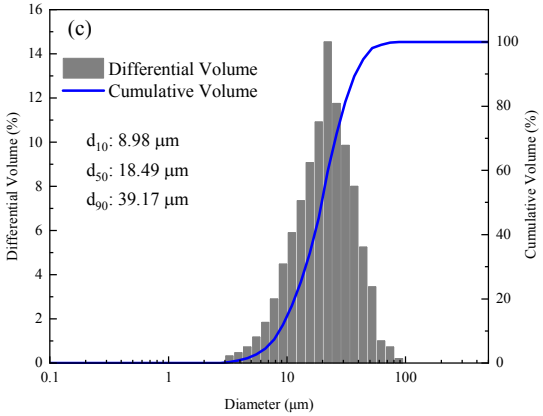

Figure 8. Particle size distribution curves of elutriated fines for different sorbents: (a) "L", (b) "LP", and (c) "L-10CA".

The particle size distributions of elutriated fines from various tests are presented in Figure 8. It can be seen that the d_{50} values of "LP" and "L-10CA" were 18.48 and 18.49 μm, respectively, obviously greater than that of "L", which is 8.74 μm. This means that the average size of elutriated fines for manufactured pellets was larger than that for natural limestone particles. The finer powders produced from natural limestone contributed to the biggest elutriation rate, presented in Figure 6. In addition, it should be noted that the d_{90} values of "LP" was 29.84 μm, evidently smaller than 39.17 μm of "L-10CA". This was due to the strengthened adhesion of powders by doping cement. It can be concluded that the prepared pellets tend to produce larger fines compared to original limestone, which is beneficial to the decline of elutriation rate.

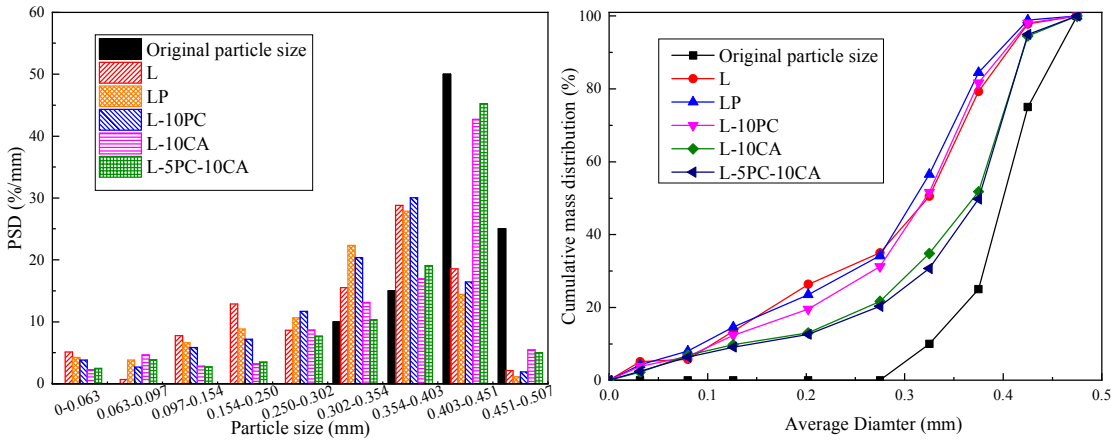

(a) PSD (b) cumulative mass distribution

Figure 9. The PSD and cumulative mass distribution of the tested sorbents after 20 cycles.

The PSD and cumulative mass distribution of four prepared pellets compared to original limestone particles are shown in Figure 9. As illustrated in Figure 9a, the

original particle sizes of all sorbents are in four ranges of 0.302-0.354, 0.354-0.403, 0.403-0.451 and 0.451-0.507 mm. After 20 cycles, a significant fraction of particles < 0.302 mm was generated. As can be seen, "L", "LP" and "L-10PC" showed a high percentage (~13-21% by mass) in 0.097-0.154 and 0.154-0.250 mm ranges, which correspond to half of the initial particle size range. This appears to be explained by the chipping attrition mechanism[34]. "L-10CA" and "L-5PC-10CA" showed major production of material in the size ranges of 0.403-0.451 and 0.451-0.507 mm (taking up 75 wt.% of original particle size), and a significant fraction of particles were generated in the range of 0.063-0.097 mm, mainly because of surface wear. This percentage was as high as 4.7% for "L-10CA", but was only 0.7% for "L". The cumulative mass distribution curve of each sample clearly decreases, as shown in Figure 9b. The changes in "L" and "LP" were most marked, meaning that the particle size for these two samples has changed more significantly after 20 multiple cycles. Doping lime-based pellets with pyrolyzed SBC or cement appears to strengthen their attrition resistance, reflected by a small movement leftward for "L-10PC", "L-10CA" and "L-5PC-10CA".

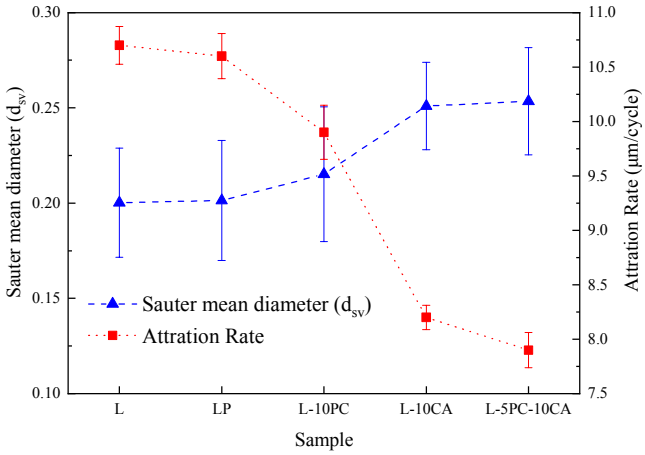

Figure 10. Sauter mean diameter and attrition rate of five sorbents after 20 cycles.

Figure 10 shows the Sauter mean diameter and attrition rate of five sorbents. The error bars represent the standard deviation between repeats. The Sauter mean diameter of the original particles is 0.415 mm, and decreased after 20 cycles to 0.254 mm ("L-5PC-10CA"), 0.251 mm ("L-10CA"), 0.215 mm ("L-10PC"), 0.201 ("LP") and 0.200 mm ("L"), with corresponding attrition rates of 7.9, 8.2, 9.9, 10.6 and 10.7 μm/cycle, respectively. It is clear that the manufactured CaO sorbents doped with pyrolyzed SBC are much more resistant to attrition than the natural limestone. Further, the attrition resistance becomes stronger after doping the pellets with cement. "L-5PC-10CA" showed the lowest attrition rate in this work.

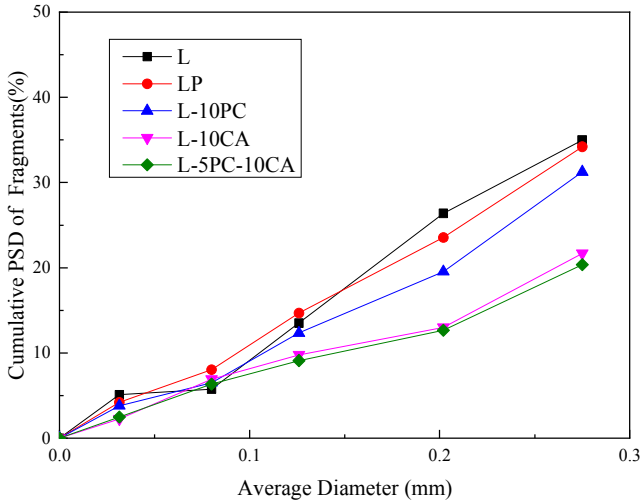

Figure 11. Breakage probability (i.e., cumulative PSD of fragments < 0.3 mm) for each sorbent.

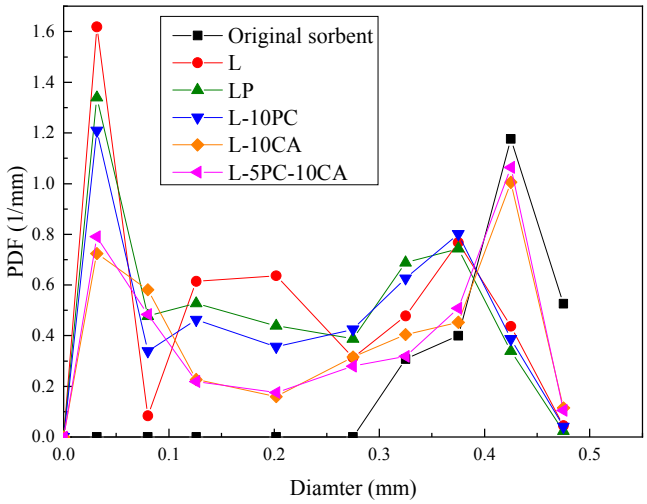

Figure 12. Probability density function (PDF) of particle size.

The probability of breakage for sorbents in BFB tests can be described by the cumulative fractional mass of fragments, measuring the particles sieved below the lower limit of the feed size interval. Here, the particles of size < 0.3 mm, were defined as fragments, and the cumulative PSDs are presented in Figure 11. After 20 cycles, the breakage probabilities for undoped sorbents were as high as 35.0% and 34.2% for "L" and "LP", respectively. The breakage probability of "L-10PC" declined to a certain extent due to the enhanced strength of SBC-doped pellets through formation of Ca_2SiO_4. By contrast, "L-10CA" indicated breakage as low as 21.7%, corresponding to 38% reduction compared to the "L" baseline sample. Accordingly, cement as support produced promising structural strength for pellets. This is especially so for the pyrolyzed SBC-doped pellets, which appear to be more attrition-resistant by adding cement simultaneously. "L-5PC-10CA" acquired the lowest breakage probability of

20.4%.

Figure 12 presents the probability density functions (PDFs) of the size of different samples after 20 cycles. The mass fraction of particles in the feed size range declined remarkably for “L” and “LP”. All samples showed distribution peaks in the 0-0.08 mm range, as a result of surface abrasion. In particular, it should be noted that there were peaks in 0.08-0.202 mm for “L”, “LP” and “L-10PC”, but not for “L-10CA” and “L-5PC-10CA”. Scala et al.[35] proposed three main particle breakage patterns, which can be reflected by PDF curves of PSD of fragments. According to this concept, “L”, “LP” and “L-10PC” experienced collisions and abrasion during reaction cycles, mostly including chipping and disintegration modes. On the contrary, “L-10CA” and “L-5PC-10CA” mostly undergo abrasion, possibly combined with moderate chipping.

Conclusions

It has been shown that the carbonation activity for pellets doped with regenerated SBC and/or cement were strongly enhanced based on TGA experiments. In this paper, BFB tests were carried out to further examine the CO_2 capture capacity and attrition properties of these pellets. The prepared pellets modified by pyrolyzed SBC and cement exhibited improved cyclic CO_2 capture capacity similar to that in TGA experiments. However, the average values were lower than those in TGA experiments, as a result of the elutriation loss of sorbents. SEM images illustrated that the prepared pellets possessed better sphericity than limestone particles, which contributed to lower elutriation rates than that of the original limestone particles. Doping pyrolyzed SBC and cement strengthened the pellet structure. “L-5PC-10CA” showed the lowest attrition rate in this work. By analyzing the probability of breakage and probability density function (PDF) of particle size for sorbents, it can be concluded that “L”, “LP” and “L-10PC” experienced significant chipping and disintegration. By contrast, “L-10CA” and “L-5PC-10CA” appear to mostly undergo abrasion. Overall, the lime-based pellets doped with both pyrolyzed SBC and cement (“L-5PC-10CA”) showed superior cyclic CO_2 capture capacity and attrition resistance. Considering the simplicity of the pyrolysis regeneration process and the excellent capture capability of pellets doped with pyrolyzed SBC and cement, the proposed system integrating CaL with SBC pyrolysis treatment appears to offer particular promise for further development at the commercial scale.

Acknowledgement

Financial support from the National Key Technology Research and Development Program of China (2016YFE0102500-06-01) is gratefully acknowledged.

References

1. Erans M, Jeremiáš M, Manovic V, Anthony EJ. Operation of a 25 KW_{th} Calcium Looping Pilot-plant with High Oxygen Concentrations in the Calciner. *J Vis Exp*. 2017;(128):1-10. doi:10.3791/56112.
2. Arias B, Diego ME, Méndez A, et al. Operating Experience in la Pereda 1.7 MW_{th} Calcium Looping Pilot. *Energy Procedia*. 2017;114:149-157. doi:10.1016/j.egypro.2017.03.1157.
3. Helbig M, Hilz J, Haaf M, Daikeler A, Ströhle J, Epple B. Long-term Carbonate Looping Testing in a 1 MW_{th} Pilot Plant with Hard Coal and Lignite. *Energy Procedia*. 2017;114(November 2016):179-190. doi:10.1016/j.egypro.2017.03.1160.
4. Hanak DP, Anthony EJ, Manovic V. A review of developments in pilot-plant testing and modelling of calcium looping process for CO_2 capture from power generation systems. *Energy Environ Sci*. 2015;8(8):2199-2249. doi:10.1039/C5EE01228G.
5. Tian S, Jiang J, Yan F, Li K, Chen X, Manovic V. Highly efficient CO_2 capture with simultaneous iron and CaO recycling for the iron and steel industry. *Green Chem*. 2016;18(14):4022-4031. doi:10.1039/C6GC00400H.
6. Alonso M, Arias B, Méndez A, Fuentes F, Abanades JC. Screening CO_2 Capture Test for Cement Plants Using a Lab Scale Calcium Looping Pilot Facility. *Energy Procedia*. 2017;114(November 2016):53-56. doi:10.1016/j.egypro.2017.03.1146.
7. Dean CC, Dugwell D, Fennell PS. Investigation into potential synergy between power generation, cement manufacture and CO_2 abatement using the calcium looping cycle. *Energy Environ Sci*. 2011;4(6):2050. doi:10.1039/c1ee01282g.
8. Rodríguez N, Murillo R, Abanades JC. CO_2 capture from cement plants using oxyfired precalcination and/ or calcium looping. *Environ Sci Technol*. 2012;46(4):2460-2466. doi:10.1021/es2030593.
9. Centi G, Perathoner S. Reduction of greenhouse gas emissions by integration of cement plants, power plants, and CO_2 capture systems. *Greenh Gas Sci Technol*. 2011;1(2011):21-35. doi:10.1002/ghg3.
10. Hanak DP, Biliyok C, Manovic V. Calcium looping with inherent energy storage for decarbonisation of coal-fired power plant. *Energy Environ Sci*. 2016;9(3):971-983. doi:10.1039/C5EE02950C.
11. Yan T, Wang RZ, Li TX, Wang LW, Fred IT. A review of promising candidate reactions for chemical heat storage. *Renew Sustain Energy Rev*. 2015;43:13-31.

doi:10.1016/j.rser.2014.11.015.
12. Chacartegui R, Alovisio A, Ortiz C, Valverde JM, Verda V, Becerra JA. Thermochemical energy storage of concentrated solar power by integration of the calcium looping process and a CO_2 power cycle. *Appl Energy*. 2016;173:589-605. doi:10.1016/j.apenergy.2016.04.053.
13. Tregambi C, Salatino P, Solimene R, Montagnaro F. An experimental characterization of Calcium Looping integrated with concentrated solar power. *Chem Eng J*. 2018;331(May 2017):794-802. doi:10.1016/j.cej.2017.08.068.
14. Cormos CC. Economic evaluations of coal-based combustion and gasification power plants with post-combustion CO_2 capture using calcium looping cycle. *Energy*. 2014;78:665-673. doi:10.1016/j.energy.2014.10.054.
15. Zhao M, Minett AI, Harris AT. A review of techno-economic models for the retrofitting of conventional pulverised-coal power plants for post-combustion capture (PCC) of CO_2. *Energy Environ Sci*. 2013;6(1):25. doi:10.1039/c2ee22890d.
16. Sun J, Liu W, Hu Y, et al. Enhanced performance of extruded-spheronized carbide slag pellets for high temperature CO_2 capture. *Chem Eng J*. 2016;285:293-303. doi:10.1016/j.cej.2015.10.026.
17. Li Y, Su M, Xie X, Wu S, Liu C. CO_2 capture performance of synthetic sorbent prepared from carbide slag and aluminum nitrate hydrate by combustion synthesis. *Appl Energy*. 2015;145:60-68. doi:10.1016/j.apenergy.2015.01.061.
18. Ma X, Li Y, Shi L, He Z, Wang Z. Fabrication and CO_2 capture performance of magnesia-stabilized carbide slag by by-product of biodiesel during calcium looping process. *Appl Energy*. 2016;168:85-95. doi:10.1016/j.apenergy.2016.01.080.
19. Sun R, Li Y, Liu C, Xie X, Lu C. Utilization of lime mud from paper mill as CO_2 sorbent in calcium looping process. *Chem Eng J*. 2013;221:124-132. doi:10.1016/j.cej.2013.01.068.
20. Miranda-Pizarro J, Perejón A, Valverde JM, Sánchez-Jiménez PE, Pérez-Maqueda LA. Use of steel slag for CO_2 capture under realistic calcium-looping conditions. *RSC Adv*. 2016;6(44):37656-37663. doi:10.1039/C6RA03210A.
21. Tian S, Jiang J, Yan F, Li K, Chen X. Synthesis of Highly Efficient CaO-Based, Self-Stabilizing CO_2 Sorbents via Structure-Reforming of Steel Slag. *Environ Sci Technol*. 2015;49(12):7464-7472. doi:10.1021/acs.est.5b00244.
22. Yan F, Jiang J, Li K, et al. Green Synthesis of Nanosilica from Coal Fly Ash and Its Stabilizing Effect on CaO Sorbents for CO_2 Capture. *Environ Sci Technol*. 2017;51(13):7606-7615. doi:10.1021/acs.est.7b00320.
23. Chen H, Khalili N. Fly-Ash-Modified Calcium-Based Sorbents Tailored to CO_2 Capture. *Ind Eng Chem Res*. 2017;56(7):1888-1894. doi:10.1021/acs.iecr.6b04234.
24. Li Y, Zhao C, Ren Q, Duan L, Chen H, Chen X. Effect of rice husk ash addition on CO_2 capture behavior of calcium-based sorbent during calcium looping cycle. *Fuel Process Technol*. 2009;90(6):825-834. doi:10.1016/j.fuproc.2009.03.013.

25. Chen H, Zhao C, Ren Q. Feasibility of CO_2/SO_2 uptake enhancement of calcined limestone modified with rice husk ash during pressurized carbonation. *J Environ Manage*. 2012;93(1):235-244. doi:10.1016/j.jenvman.2011.08.023.
26. Su C, Duan L, Donat F, Anthony EJ. From waste to high value utilization of spent bleaching clay in synthesizing high-performance calcium-based sorbent for CO_2 capture. *Appl Energy*. 2018;210(August 2017):117-126. doi:10.1016/j.apenergy.2017.10.104.
27. Erans M, Beisheim T, Manovic V, et al. Effect of SO_2 and steam on CO_2 capture performance of biomass-templated calcium aluminate pellets. *Faraday Discuss*. 2016:97-111. doi:10.1039/C6FD00027D.
28. Duan L, Yu Z, Erans M, Li Y, Manovic V, Anthony EJ. Attrition Study of Cement-Supported Biomass-Activated Calcium Sorbents for CO_2 Capture. *Ind Eng Chem Res*. 2016;55(35):9476-9484. doi:10.1021/acs.iecr.6b02393.
29. Yu Z, Duan L, Su C, Li Y, Anthony EJ. Effect of steam hydration on reactivity and strength of cement- supported calcium sorbents for CO_2 capture. *Greenh Gases Sci Technol*. doi:10.1002/ghg.1690.
30. Duan L, Su C, Erans M, Li Y, Anthony EJ, Chen H. CO_2 Capture Performance Using Biomass-Templated Cement-Supported Limestone Pellets. *Ind Eng Chem Res*. 2016;55(39):10294-10300. doi:10.1021/acs.iecr.6b02965.
31. Manovic V, Anthony EJ. Long-term behavior of CaO-based pellets supported by calcium aluminate cements in a long series of CO_2 capture cycles. *Ind Eng Chem Res*. 2009;48(19):8906-8912. doi:10.1021/ie9011529.
32. Knight A, Ellis N, Grace JR, Lim CJ. CO_2 sorbent attrition testing for fluidized bed systems. *Powder Technol*. 2014;266:412-423. doi:10.1016/j.powtec.2014.06.013.
33. Ray YC, Jiang TS, Wen CY. Particle attrition phenomena in a fluidized bed. *Powder Technol*. 1987;49(3):193-206. doi:10.1016/0032-5910(87)80128-6.
34. Materic V, Holt R, Hyland M, Jones MI. An internally circulating fluid bed for attrition testing of Ca looping sorbents. *Fuel*. 2014;127:116-123. doi:10.1016/j.fuel.2013.10.071.
35. Scala F, Montagnaro F, Salatino P. Attrition of limestone by impact loading in fluidized beds. *Energy and Fuels*. 2007;21(5):2566-2572. doi:10.1021/ef0700580.

CO2 capture and attrition performance of competitive eco-friendly calcium-based pellets in fluidized bed

Su, Chenglin

2018-11-15

Su C, Duan L, Anthony EJ. (2018) CO2 capture and attrition performance of competitive eco-friendly calcium-based pellets in fluidized bed. Greenhouse Gases: Science and Technology, Volume 8, Issue 6, December 2018, pp. 1124-1133

10.1002/ghg.1825